Publ. Astron. Obs. Belgrade No. 73 (2002), 231 - 246 *Poster*

R-BAND PHOTOMETRIC PROFILES OF 120 EDGE-ON NORTHERN GALAXIES

O. I. STANCHEV, Ts. B. GEORGIEV, and Yu. B. GORANOVA
Institute of Astronomy, Bulgarian Academy of Sciences
72 Tsarigradsko Shosse, 1784 Sofia, Bulgaria
E-mail stanchev@astro.bas.bg

Abstract. The major and minor axis profiles of 120 late type edge-on galaxies, observed with the 6-m telescope in the R band, are presented. Only 7 of them ($\sim 6\%$) show exponential shapes, 99 ($\sim 83\%$) have well pronounced truncation below 24 mag/arcsec^2 and 13 ($\sim 11\%$) are intermediate, with weak truncation below 25 mag/arcsec^2. A brief survey of the possible explanation of the truncation effect is given. The major-axis sizes and axial ratios at 25 mag/arcsec^2, as well as the respective Tully–Fisher relations are presented. The "edge-on" TF relations may be used as raw distance estimators, having relative standard errors $25 - 33\%$.

1. INTRODUCTION

The investigation of the distribution of stars in galaxies is very important for elucidation of their structure and evolution. Surface photometry provides information about the space distribution of stars in the galactic bulges and disks, if galaxies under various projection angles (inclinations, i) are compared. In this sense the edge-on galaxies, having $i \approx 90°$, are very valuable. They show the galactic structures perpendicular to the galactic plane and give possibility to disentangle the components that have different scale parameters. In addition, due to the line-of-sight integration, one can follow the light distribution to large distances from the center. One very interesting fact is that most of the edge-on galaxies show strong truncation of their major axes profiles. Here we present and discuss a uniform system of profiles and sizes of such galaxies.

2. THE PROFILES AND THEIR CLASSIFICATION

In this work we use the smoothed profiles of 120 northern edge-on galaxies, derived from the isophote maps of Karachentsev et al. (1992). The sample is selected from the reprints of the POSS by the criterion "axial ratio on blue photographs $a/b > 7$ and contains almost all such galaxies with major axis $2 < a < 8$ arcmin. Observations had been carried out with the 6-m telescope with CCD-camera attached to the focal reducer in 1988–1990. The photometry has been performed in red bandpass, close to the R-system of Cousins ($\lambda_{\rm eff} \approx 6500$ Å). Using the table of Karachentsev et al.

(1992), we list the basic data on the galaxies, as well as the parameters derived by us in Table 1, as follows:

– UGS – galaxy number in the Uppsala General Catalogue;
– V – radial velocity in km/s, with respect to the Local Group (this work);
– W – 21 cm FWHM line-width in km/s;
– m_{24}^0 – extinction corrected magnitude (R) within the isophote 24 mag/arcsec^2 (this work);
– α_{25} – angular radius in arcsec along the major axis at 5 mag/arcsec^2 (this work);
– α_{25}/b_{25} – apparent aspect ratio at 25 mag/arcsec^2 (this work);
– M – absolute magnitude of the galaxy, calculated with m_{24}^0 (this work);
– A – galaxy linear diameter in kpc, corresponding to $2\alpha_{25}$;
– PT – profile type: e – exponential, t – truncated, i – intermediate;
– WP – warp presence (w);
– HP – halo presence (h).

Most of the large late-type disk galaxies, which are visible edge-on, show strong deviation from the expected exponential brightness shape, i.e. their photometric profiles seem to be truncated. A statistical study of this truncation may pose interesting constraints on galaxy formation theory. For example, if the truncation were also present in the mass distribution, it would have important dynamical consequences at the discs outer edges. From this point of view we classified empirically the shapes of the major axis profiles of the sample galaxies in *three types* - exponential, truncated and intermediate:

– *Exponential profiles* with long quasi-linear parts up to 25–26 mag/arcsec^2 have 7 galaxies ($\sim 6\%$).

– *Truncated profiles* with strong decrease of the surface brightness below 24 mag/arcsec^2 have 99 galaxies ($\sim 83\%$).

– *Intermediate profiles* with linear part and weakly pronounced truncation after 25 mag/arcsec^2 have 13 galaxies ($\sim 11\%$).

One galaxy (UGC 9556) has been classified as peculiar (see Sect. 3).

Examples of the profiles are shown in Fig. 1. Figure 5 presents the smoothed profiles of all 120 edge-on galaxies from the sample.

The truncations (cut-offs) are placed at low surface brightness levels, as it is seen from the profiles in Fig. 1. These cut-offs are not infinitely sharp edges, but rather regions where the radial exponential scale length suddenly decreases from several kpc to less than ~ 1 kpc.

There are many suggestions as to the causes of such cut-off effects at the edges of the disks of most edge-on galaxies. For example, Bottema (1995) suggests that tidal interactions between neighboring galaxies may be the cause of sharp disk truncation in individual galaxies. Another possible explanation of the truncations is that star formation has ceased at that position due to the low H I density (Fall & Efstathiou 1980; van der Kruit & Searle 1981). But in scenario with slow disk formation (Larson 1976) the truncation radius might be the radius where the disk formation time equals the present age of the galaxy formation mechanisms.

Generally, we must include both intrinsic physical processes and projection effects due to the positions of spiral arms with respect to the line-of-sight. The importance of the latter effects can be assessed observationally, since in this case one would expect an asymmetry in either of the truncations themselves on either side of the galaxy.

Table 1: Some basic data on the sample of 120 edge-on galaxies

UGC	V	W	m^0_{24}	α_{25}	$(\alpha/b)_{25}$	M	A	PT	WP	HP
231	841	210	12.70	141.3	6.9	-17.96	18.59	e		
290	758	100	15.99	49.6	4.6	-14.46	5.90	i	w	
418	4438	382	13.64	63.05	4.19	-20.27	36.91	t		
485	5238	359	13.57	77.4	4.8	-20.74	54.76	t	w	
507	5277	455	13.17	73	3.5	-21.07	49.90	t	w	h
542	4508	368	13.04	61.7	2.9	-20.96	37.72	t		h
711	1978	202	13.96	113.15	7.05	-18.12	28.58	e		
1400	5536	963	11.73	87.8	2.8	-22.70	65.42	t		h
1650	4585	235	15.41	36.4	3.2	-18.63	22.67	e		
1839	1535	142	14.46	65.3	4.4	-16.98	12.28	t	w	h
1867	5195	281	13.97	62.6	5.4	-20.36	44.42	t		
1970	1915	228	13.60	70.1	3.5	-18.59	18.56	t		h
2092	6120	452	13.72	96.9	4.2	-20.83	76.50	t		h
2101	5835	500	13.36	64.5	3.9	-21.20	50.91	t		h
2370	2162	194	14.62	67.8	7.7	-17.94	21.34	t		
2411	2546	312	13.07	140.3	10.6	-19.85	52.11	i		
3326	4085	528	12.91	111.2	6.2	-21.02	65.81	t		
3365	5150	537	12.64	66	3.5	-21.73	47.74	t		h
3425	4057	419	12.94	138	4.4	-20.96	80.38	i		h
3474	3633	360	12.97	75.1	4.3	-20.72	39.86	t		
3489	5455	475	13.65	65.9	5.3	-20.79	49.40	t	w	
3539	3305	312	13.98	67	4	-19.49	32.08	t		h
3597	5958	-	13.45	61.3	3.5	-21.19	50.41	e	w	
3697	3136	262	12.99	107.6	9.95	-20.43	50.29	t	w	
3782	2269	336	12.56	115.4	4.9	-20.19	39.71	t	w	
3879	4797	250	14.56	67	3.9	-19.64	45.05	i	w	
3959	3109	425	12.28	119	4.6	-21.08	54.19	i	w	h
4043	3401	419	13.46	73.5	3.9	-20.09	36.46	t		
4148	736	135	15.67	54.9	5.2	-15.28	8.24	t	w	
4257	4164	243	14.66	69.4	5.2	-19.28	41.24	t	w	
4259	3832	397	13.09	64.7	3.4	-20.72	36.20	t		h
4277	5459	575	13.13	122	4.4	-21.35	93.00	i		h
4278	563	180	12.50	146.3	6.5	-18.11	18.82	t		h
4550	2068	264	13.76	84.2	3.6	-18.89	27.70	t		h
4704	596	129	14.32	120.8	5.25	-16.38	16.17	i	w	
4719	5116	542	13.13	80.9	4.9	-21.22	58.14	t	w	
4961	1578	324	12.67	111.3	4.8	-19.53	29.63	t		
5173	6237	491	13.64	86.9	5.4	-21.14	75.91	t	w	h
5203	1551	190	14.22	79.9	5.4	-18.01	21.56	t	w	
5210	4441	304	14.19	66	4.2	-19.90	42.16	t	w	
5341	7568	607	13.85	97.3	7	-21.31	101.28	t		
5389	6980	352	14.55	65.6	5.5	-20.42	62.86	t		
5452	1342	200	13.59	79.65	4.5	-18.29	18.37	t	w	
5495	8249	569	13.55	81.9	3.3	-21.78	92.72	t	w	h
5537	3756	288	14.40	80.25	5	-19.40	44.85	i		h
5662	1324	173	14.18	102.6	6.9	-17.69	23.53	e	w	
5687	3563	258	14.27	66.6	4.2	-19.45	35.72	t	w	
5741	1391	325	12.46	95.3	3.8	-19.61	24.01	t		h

Table 1: (continued)

UGC	V	W	m^0_{24}	α_{25}	$(\alpha/b)_{25}$	M	A	PT	WP	HP
6080	2180	190	14.97	59	4.06	-17.79	20.42	t		
6116	1134	304	12.31	125.6	5.3	-19.41	26.83	t		
6483	3891	324	13.74	56.2	3.6	-20.12	32.20	t		
6497	6324	384	14.74	63.8	4.9	-20.02	55.45	t		
6594	1040	171	14.05	79.2	4.2	-17.60	16.38	t	w	
6667	978	176	13.47	100.6	5.8	-17.97	18.87	t	w	
6686	6546	402	13.77	89	5.4	-21.12	81.83	t	w	
6774	2417	228	14.05	57.8	4.6	-18.90	21.75	i	w	
6802	1256	139	14.16	70.2	4.2	-17.66	15.75	t	w	
7001	1507	196	13.55	84.15	5.3	-18.74	23.37	t	w	h
7153	2606	264	14.28	67.7	4.8	-18.83	27.54	t		
7170	2444	210	14.11	87.6	5.7	-18.92	34.34	t	w	
7222	931	232	12.02	138	4.1	-19.31	24.60	t		h
7279	1978	208	14.33	73	5.2	-18.46	25.56	t		h
7291	226	218	12.43	106.4	4.3	-18.04	12.78	t		h
7301	712	131	14.39	53.3	4.7	-16.60	8.15	t	w	
7313	2131	214	13.86	68.3	4.6	-19.04	25.13	t		
7321	409	210	12.99	160.3	10.5	-17.48	19.29	t		
7387	1733	256	13.91	72	5.3	-18.74	23.57	t		h
7403	2541	363	12.70	112.6	4.1	-20.54	48.70	t		h
7459	525	189	13.84	72.7	4.6	-16.50	8.26	t	w	
7513	995	280	12.21	124.2	4.9	-19.68	28.76	t		
7522	1428	310	12.70	87.7	4.7	-19.69	25.50	t		h
7607	4226	278	14.67	104.25	6.3	-19.47	68.05	t		h
7617	6972	436	14.06	80.1	5.2	-20.92	77.14	t	w	h
7687	1733	144	14.02	81.4	4.4	-18.66	27.12	t		
7725	1759	151	13.55	80.4	3.8	-19.16	27.13	e	w	
7774	526	190	13.78	97.8	5.6	-16.82	12.51	t		
7808	7273	520	13.91	98.9	5.3	-21.26	103.44	i		
7993	4789	366	14.27	65.7	4.9	-19.99	45.38	t	w	
7999	4761	442	13.22	64.4	4.2	-21.00	43.39	t		
8025	6316	513	13.33	63.3	4.4	-21.47	56.00	t		
8146	669	162	13.44	99.9	5	-17.68	16.19	t		
8286	407	179	12.01	159.9	5.3	-18.62	20.72	t		
8463	4647	-	12.65	82.5	4.3	-21.65	58.04	t		h
8115	2049	256	13.08	67.5	4.3	-19.63	22.71	t		
9127	2883	570	11.85	131.9	6.8	-21.63	63.57	t		
9242	1440	187	13.63	136.5	10.1	-18.77	39.95	i	w	
9249	1365	147	14.46	69	4.7	-18.08	21.58	t		
9422	3310	314	13.93	62.2	5.3	-19.76	33.05	t		
9431	2237	330	12.93	99.5	5.2	-20.10	38.75	t		
9556	2292	230	14.88	45	4.1	-18.12	17.39	i		h
9568	2138	418	12.49	110.4	3.5	-20.41	40.60	t		h
9760	2015	144	14.91	94.05	5.8	-18.16	37.51	t		
9780	5178	335	14.04	71.5	4	-20.48	55.55	t	w	h
9856	2491	218	14.62	90	4.8	-18.64	39.11	t		h
9948	2612	536	12.37	94.2	4	-20.88	40.78	t	w	
9977	1912	247	13.35	111.6	5.9	-19.65	42.98	t		h

Table 1: (continued)

UGC	V	W	m^0_{24}	α_{25}	$(\alpha/b)_{25}$	M	A	PT	WP	HP
10227	9026	600	13.84	74	5	-21.77	95.10	t	w	
10288	2045	352	12.69	146.9	5.3	-20.40	58.88	i		h
10297	2306	224	13.98	67.5	4.4	-19.25	28.98	t		
11132	2828	339	13.85	65.5	3.7	-19.60	31.19	t	w	
11230	7103	400	14.57	65.25	4.4	-20.52	65.84	t		
11301	4500	491	12.69	88.1	6	-21.59	61.40	t	w	
11394	4236	365	13.47	71.25	5.1	-20.68	46.70	t	w	
11411	7438	396	14.19	69	4.3	-20.99	72.67	t	w	
11838	3478	250	14.08	66	5.2	-19.57	34.30	t		h
11841	5989	535	12.90	98.4	6.9	-21.81	83.26	t		
11859	3014	306	14.18	74.6	5	-19.18	33.96	e		h
11893	5564	619	13.18	78.1	3.9	-21.37	61.55	t		
11964	1399	170	14.75	64.4	5.8	-17.25	15.65	t	w	
11994	4872	404	13.03	64.9	4	-21.24	45.04	t		
12001	4269	534	12.84	71.6	4	-21.18	44.16	t		
12190	7263	577	13.54	71.6	4.7	-21.52	71.19	t	w	h
12281	2567	260	13.34	105.1	6.6	-19.62	39.81	t		
12411	8656	571	13.25	54.4	5.4	-22.17	64.15	t		
12423	4838	486	13.08	114.4	4.9	-21.10	76.13	i		h
12430	3676	225	13.54	81.75	5.3	-20.13	42.90	t	w	
12452	4960	314	14.01	69	4.2	-20.22	46.90	t	w	h
12506	2385	345	13.47	88	4.4	-19.32	30.78	t		
12693	4952	220	14.79	58.5	5	-19.46	40.15	t	w	
12900	6803	458	14.09	71.25	4.75	-20.77	64.91	t	w	

3. SOME PECULIARITIES

We find weak halos in 40 ($\sim$ 33%) of the examined galaxies. The most prominent of them – UGC 5495 – is shown in Fig. 2 (left panel).

Many galaxies, including our own, show large-amplitude warps in the outer parts of their disks. Departures from the ideal symmetry involve warps, tilts, corrugations, differential ellipticity, vertical convection with the halo, etc. Flaring, even if it does not break the ideal disk symmetry, may again be considered a perturbative effect. These features are not large but are common. Their study may provide clues to understanding the nature of galaxies and the intergalactic medium.

We noticed warping features in 47 of our 120 sample galaxies ($\sim$ 39%). Figure 2 (right panel) presents image of an S-shaped edge-on galaxy – UGC 3697.

We also have one galaxy – UGC 9556 – with profile, showing big bulge and long exponential periphery as it appears in Fig. 3. It is possible, that these peculiarities in the profile shape are due to bad photometric calibration.

4. TULLY–FISHER RELATIONS

The Tully–Fisher (TF) relations are important tools for distance estimation in the

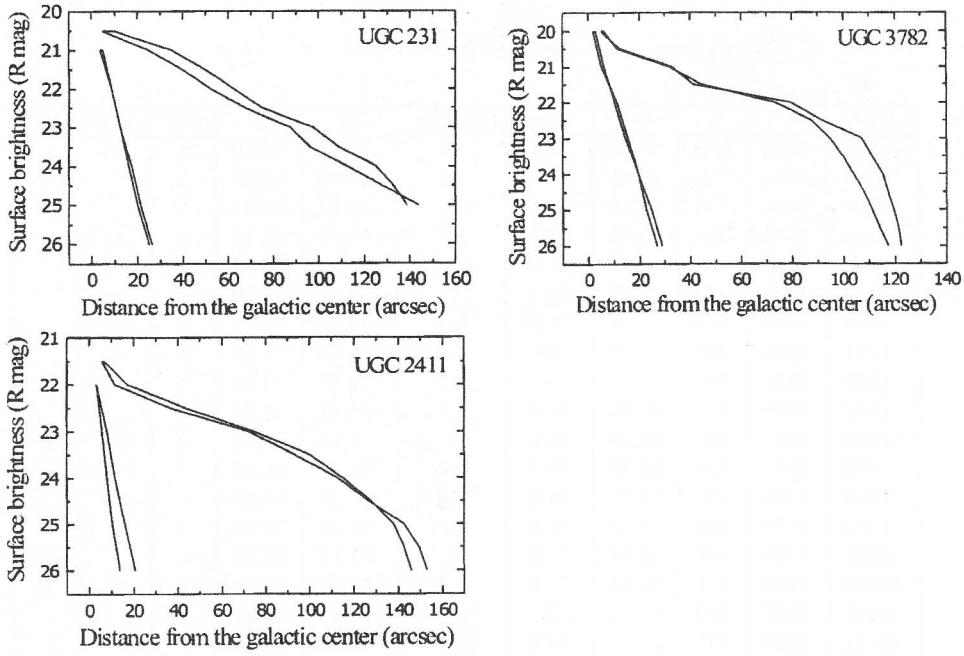

Fig. 1: Photometric profiles of UGC 231 (exponential, the left top panel), UGC 3782 (truncated, the right top panel) and UGC 2411 (intermediate, the bottom panel).

Universe. Due to the errors of the inclination estimation, the corrections of the observed sizes or magnitudes of the galaxies to face-on view increases the scatter of the relations. However, in the special case of edge-on galaxies these corrections may be omitted. Then we must expect that the "edge-on" Tully–Fisher relations for the later giant galaxies must be narrower than the usual ones.

Figure 4 (left panel) presents the TF relations between the absolute magnitude M and the 21 cm FWHM linewidth W (km/s) for 107 galaxies. Because of the absence of data on W, two galaxies (UGC 3597 and UGC 8463) are not included in this relation. Moreover, we consider the galaxies UGC 290, UGC 4148, UGC 7301 and UGC 7459 with $M > -16$ mag, as probably nearby dwarfs. They are excluded, too. Besides, the galaxies UGC 3425, UGC 7607, UGC 7774, UGC 9127, UGC 11301, and UGC 11411 are also excluded because of their bad frames. The galaxy UGC 1400 does not participate in the relation because in PGC it is classified as a "multiple" galaxy.

The absolute magnitude M was calculated from the equation

$$M = m^0{}_{24} - 25 - 5 \lg V + 5 \lg H_0. \qquad (1)$$

Using the relations $A_R = 0.57 A_B$ and $m^0_{24} = m_{24} - A_R$, m^0_{24} in Eq. (1) is the extinction corrected red (R) magnitude within the isophote of 24 mag/arcsec^2. We use the data about A_B from the Revised Flat Galaxy Catalogue of Karachentsev et al. (1999) and the Lyon/Meudon Extragalactic Database (LEDA). $H_0 = 75$ km s^{-1} Mpc^{-1} is the adopted Hubble constant. V is the radial velocity in (km/s)

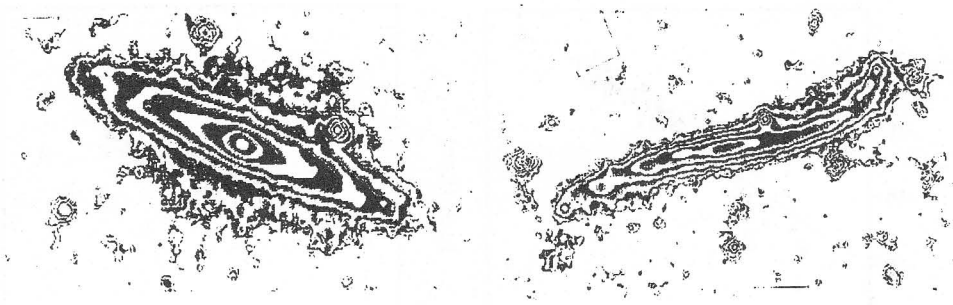

Fig. 2: The isophote maps of UGC 5495 (left panel) and the warped galaxy UGC 3697 (right panel)

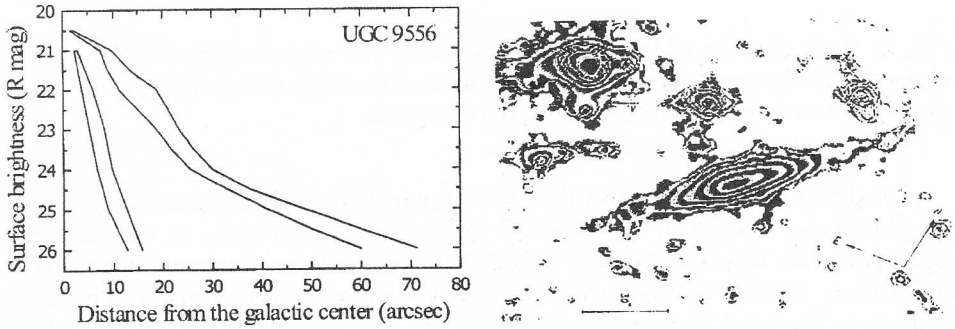

Fig. 3: Photometric profile of UGC 9556 (left panel) and its isophote map (right panel)

corrected from heliocentric to Local Group, through a method recommended by the NASA/IPAC Extragalactic Database, based on the work of Karachentsev & Makarov (1996). Figure 4 (right panel) presents the TF relation between the linear diameter A (kpc) and W (km/s) for the same 107 galaxies. Here the same galaxies as these in the previous TF relation are excluded. We calculate the linear diameter of an observed galaxy from the equation

$$A_{25} = 2a_{25}\frac{V}{H_0}1000, \tag{2}$$

where α_{25} is the galaxy angular radius along the major axis at 25 mag/arcsec^2 converted in radians.

In Fig. 4 (left panel) the data are fitted with the line

$$M = \begin{array}{l} -3.13 - 6.70\lg W, \\ \pm 0.64 \pm 0.26 \end{array} \qquad \sigma_M = 0.4771,$$

and for Fig. 4 (right panel) – with the line

$$\lg A = \begin{array}{l} -0.91 + 1.00\lg W, \\ \pm 0.17 \pm 0.07 \end{array} \qquad \sigma_{\lg A} = 0.1237.$$

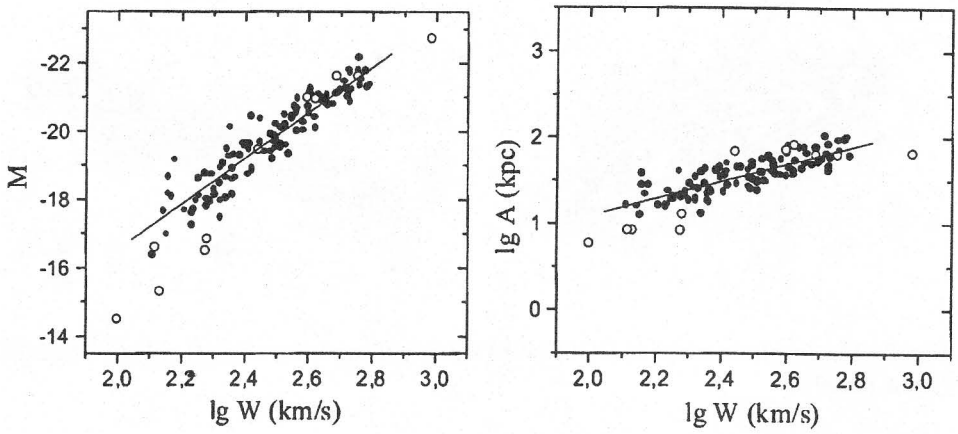

Fig. 4: Two variants of the TF relations about 107 edge-on galaxies. The vertical scales of the two panels are set in such a way that the scale of the dispersion in relative distance error is visually the same in the two cases.

For the same TF relation as this in the left panel but without extinction correction, we obtain $\sigma_M = 0,4818$. As it seems the extinction correction in our case is not significant, but this is so because the galaxies have not very large extinction as seen in Table 1. Besides that, if in this TF relation we use absolute magnitude M with respect to the total blue visual magnitude B_t^0 (taken from RFGC and LEDA, and corrected for extinction) instead of with respect to the visual magnitude in R-light, then we could obtain $\sigma_M = 0.6593$.

Let us compare the two TF relations as distance estimators. The distance modulus standard errors are $\sigma_\mu = \sigma_M = 0.48$ mag and $\sigma_\mu = 5\sigma_{\lg A} = 0.62$ mag, respectively. The corresponding relative distance errors are $10^{\sigma_\mu/5}$, i.e. $25 - 33\%$, respectively.

A previous investigation of 117 galaxies of the present sample, based on less accurate data, shows badly defined TF relations. The scatters of the relations of type (1) in the B-band and (2) in the R band are $0.75 - 0.85$ mag (relative distance error is $40 - 50\%$) (Georgiev 1992). In the present paper we use more accurate CCD data and because of this the scatters of the TF relations grow down ~ 1.5 times.

5. CONCLUSIONS

We show that 83% of the studied edge-on galaxies have strongly truncated major axis profiles. Because of their large apparent sizes a few edge-on galaxies (NGC 891, NGC 4244, NGC 5907, etc.) with known truncated profiles are not included in the discussed sample. Another homogenous sample of southern edge-on galaxies is investigated by Pohlen et al. (2000). Applying our classification for the galaxies in this sample, we found that 28 of them have truncated profiles and only 3 galaxies (ESO 319-026, ESO 578-025 and ESO 583-008) may be considered as belonging to the intermediate type. Therefore, the standard exponential disk model must be revised. Generally, we conclude that $\sim 90\%$ of the disk edge-on galaxies have truncated profiles. Further we show that the "edge-on" TF relations may be used as raw distance estimators, having

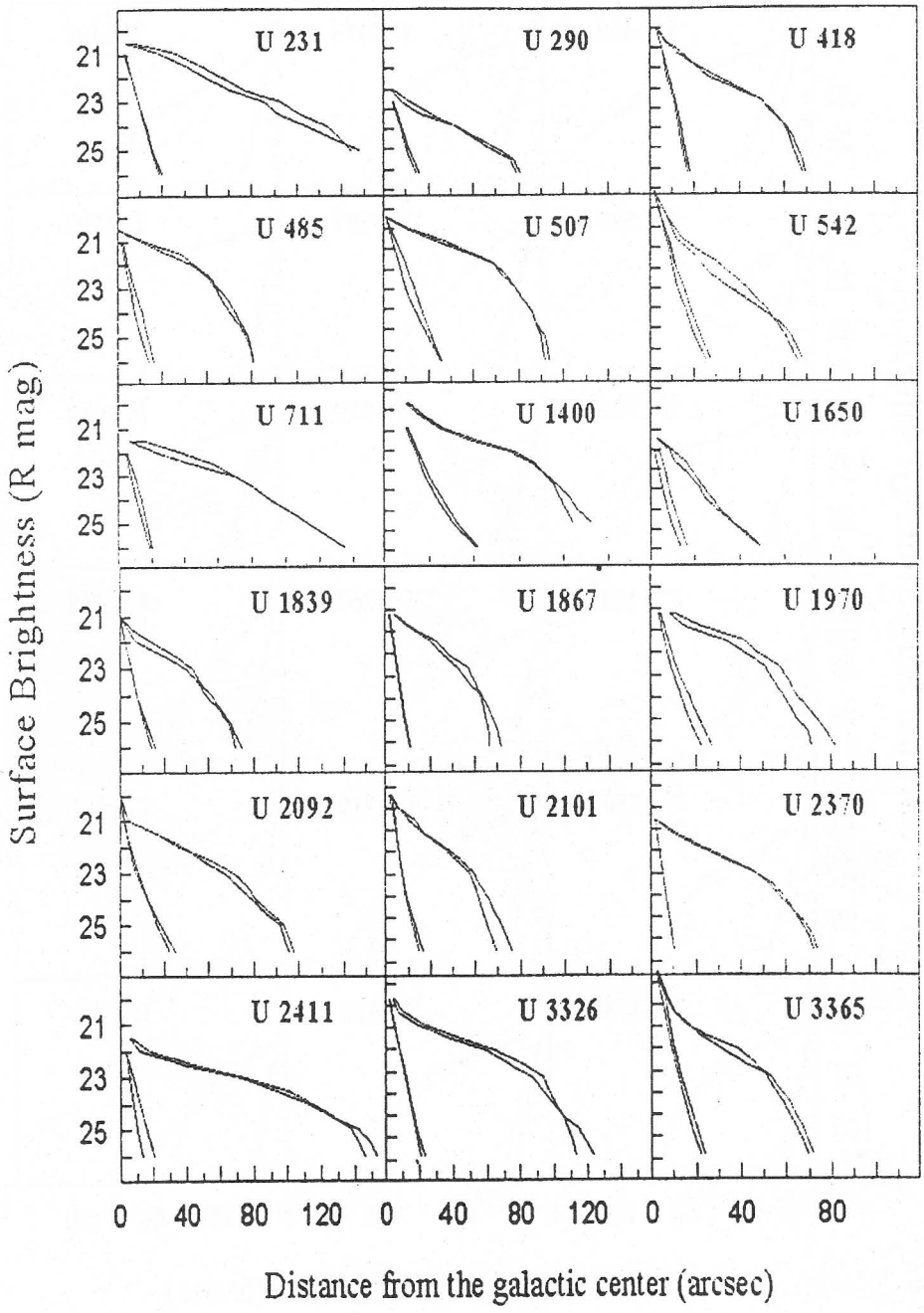

Fig. 5: Smoothed photometric profiles for the sample of 120 edge-on galaxies.

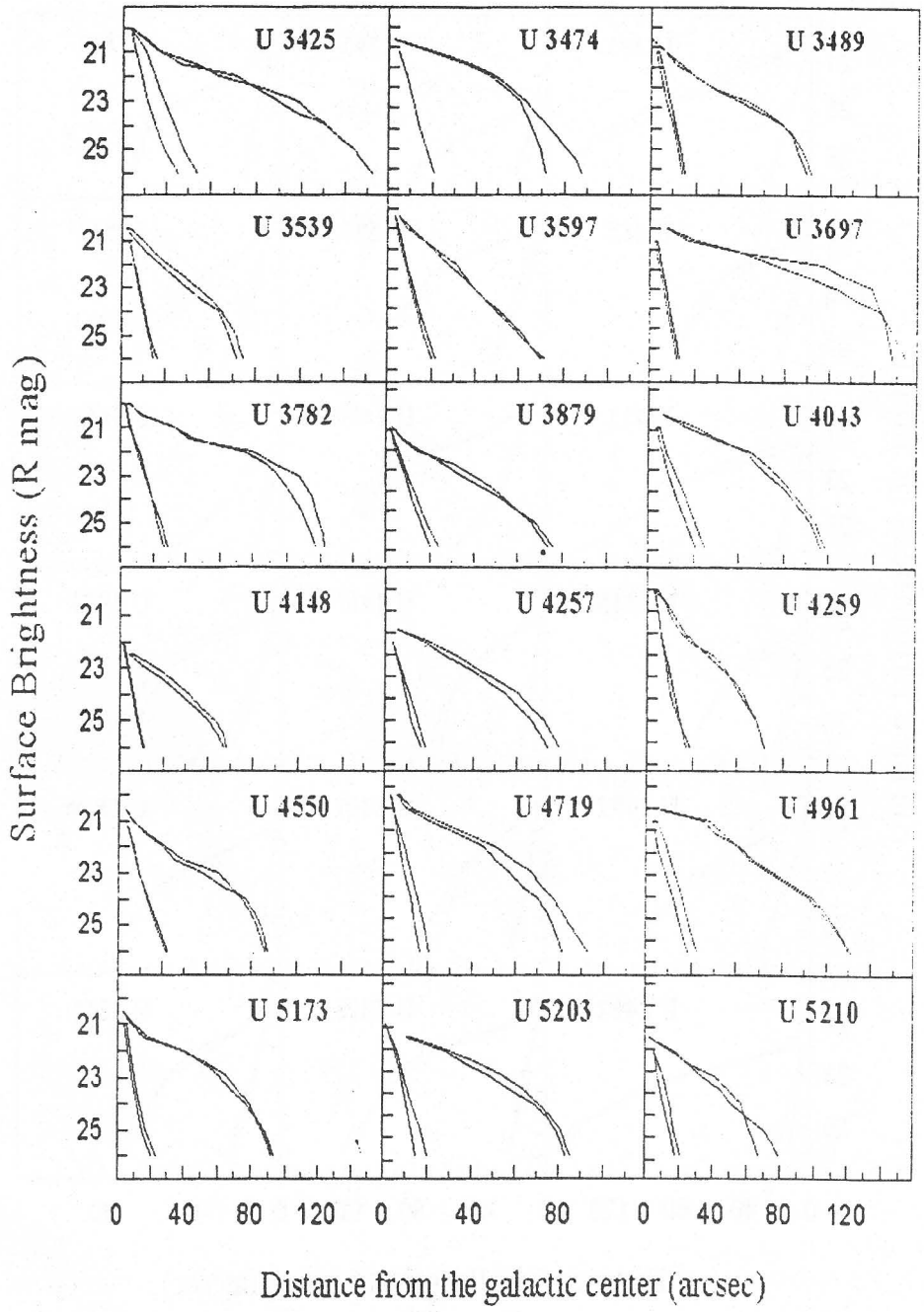

Fig. 5: (continued)

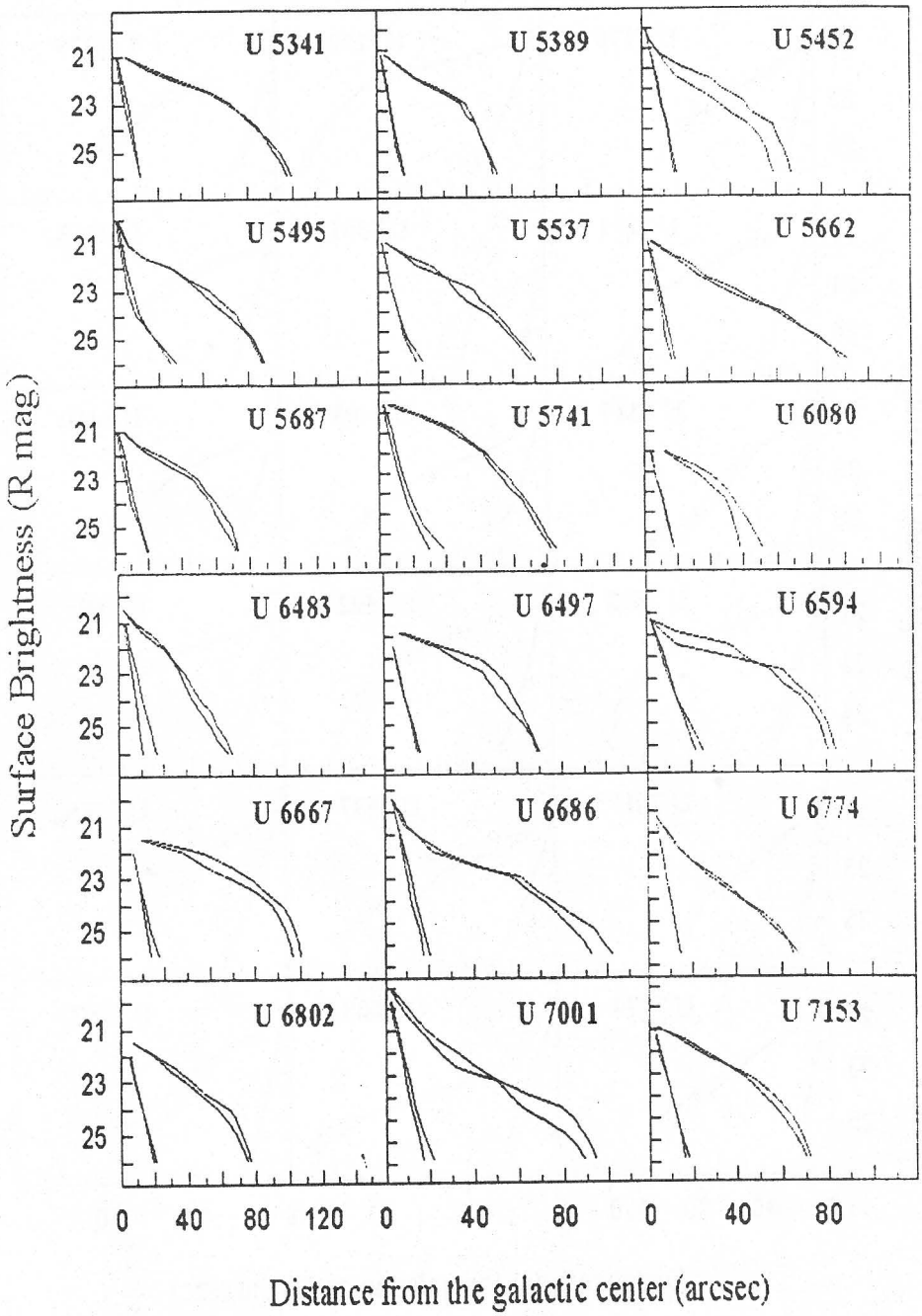

Fig. 5: (continued)

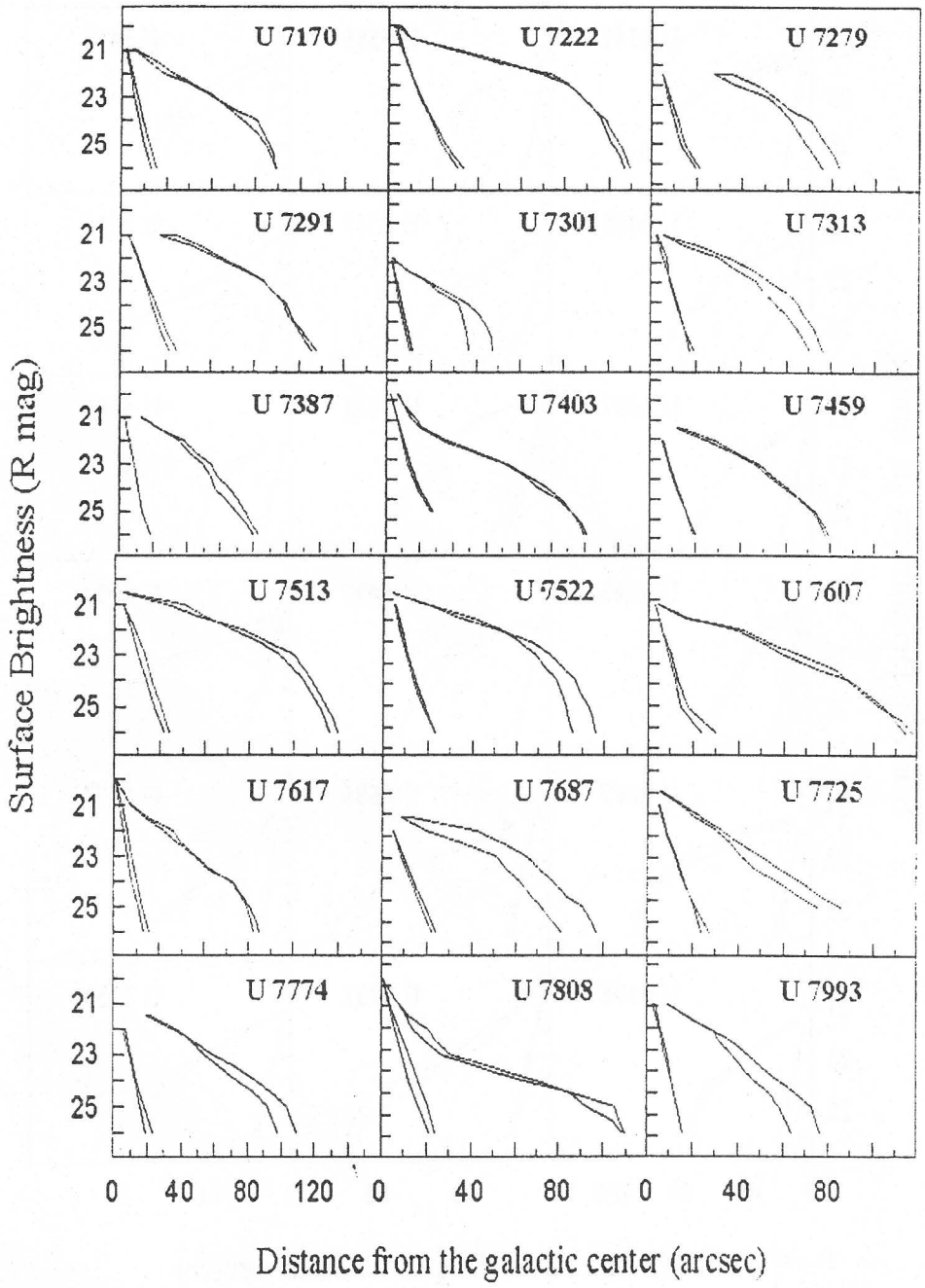

Fig. 5: (continued)

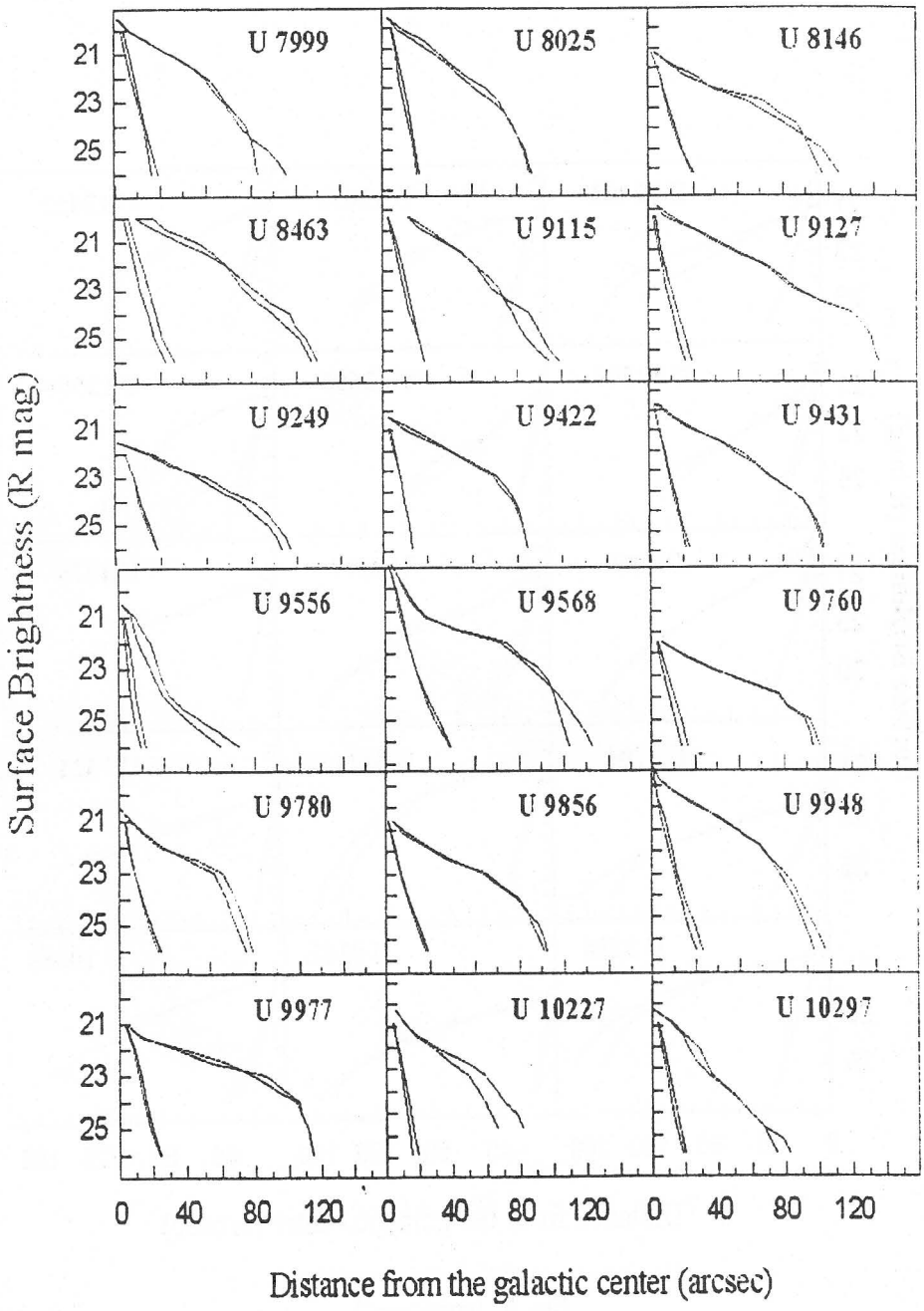

Fig. 5: (continued)

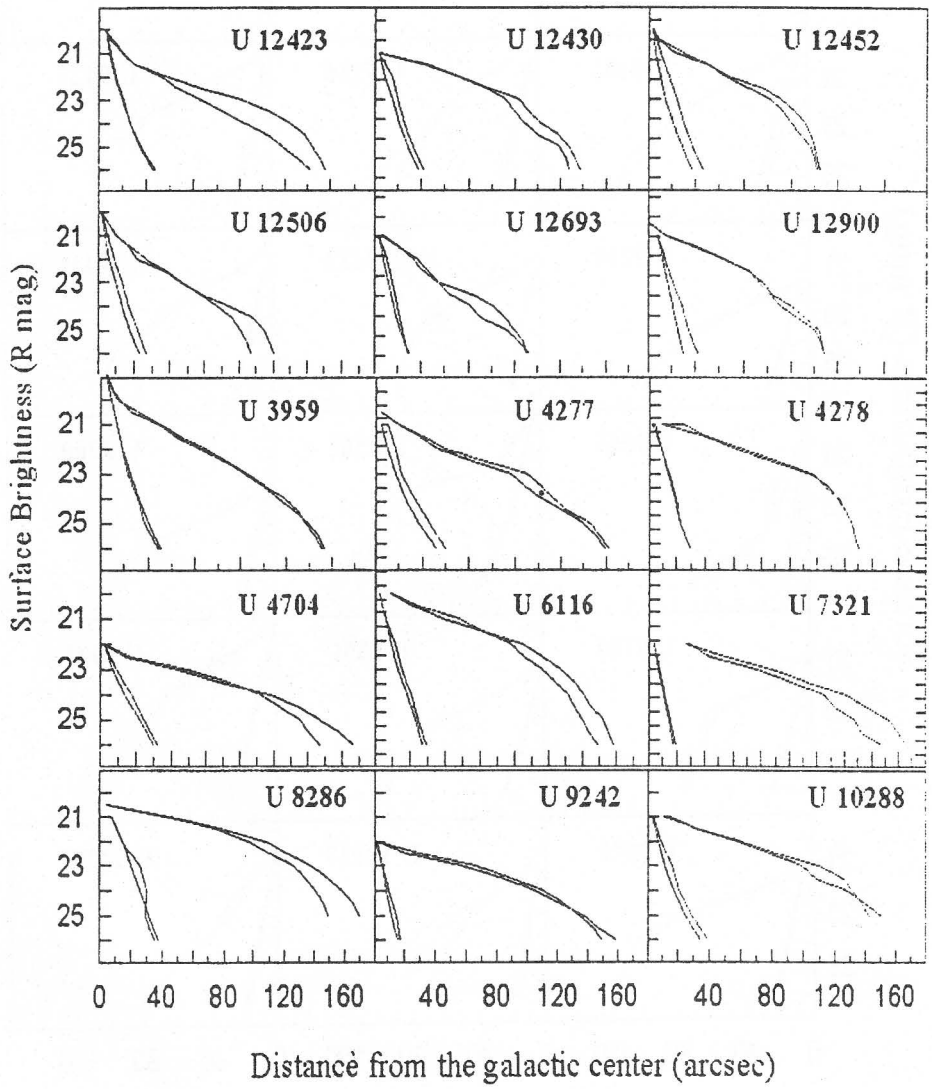

Fig. 5: (continued)

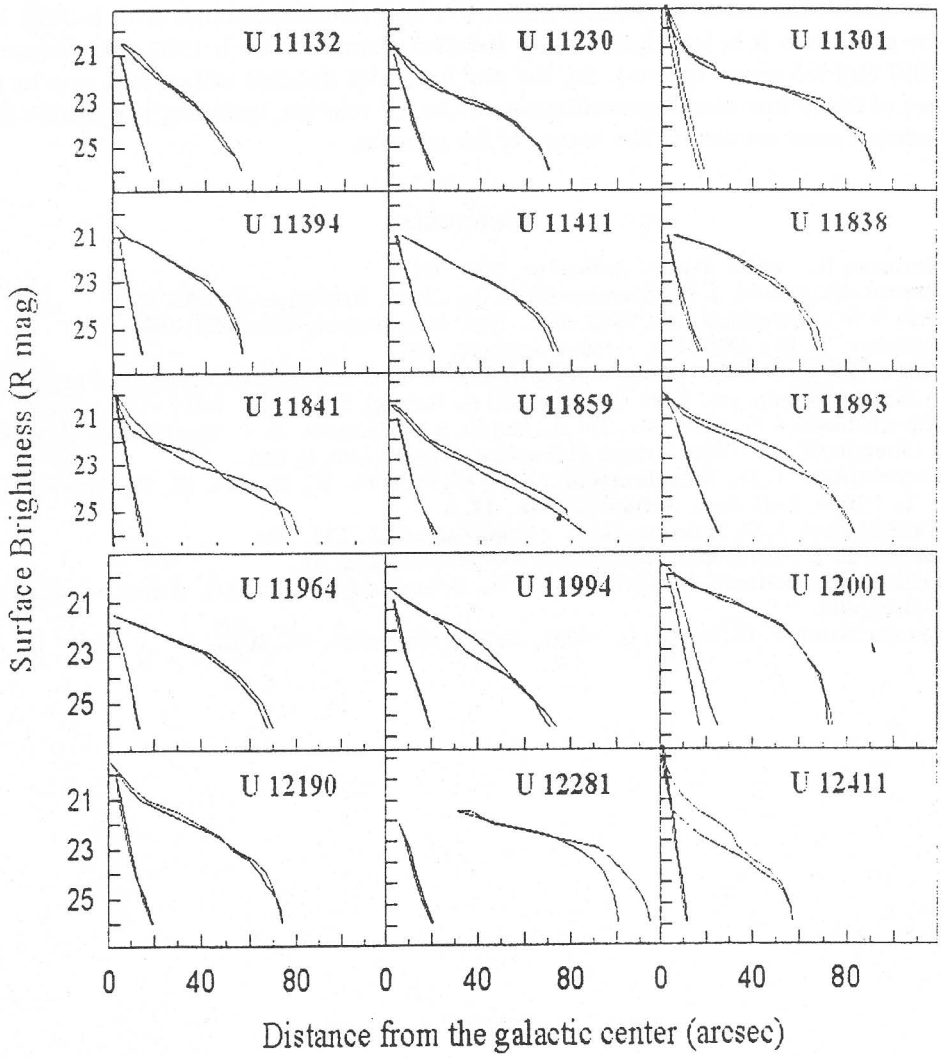

Fig. 5: (continued)

relative standard errors about 30%.

Generally, the scatter of the TF relations arises from four main sources – errors in the measurements of the parameters, uncertainties associated with the corrections applied to them, variance of the galactic properties and the Malmquist bias of the sample. The mean apparent scatter of the I band TF relation, in the case of galaxies in clusters, is typically about 0.4 mag (Bureau et al. 1996). It is known also, that in the scatter for the small galaxies exceeds 0.5 mag (relative distance error is 30%) and for giant ones it is less than 0.3 mag (relative distance error is 15%) (see Giovanelli 1997 and references therein). So, the way for better distance estimations may be the use of multidimensional generalization of the TF relation, including parameters that account more accurately the nature of the galaxies.

References

Bottema, R. : 1995, *Astron. Astrophys.*, **295**, 605.

Bureau, M., Mould, J. R., Staveley-Smith, L. : 1996, *Astrophys. J.*, **463**, 60.

Fall, S. M., Efstathiou, G. : 1980, *Mon. Not. Royal Astron. Soc.*, **193**, 189.

Georgiev, T. B. : 1992, *Sov. Astron. Lett.*, **18**, 299.

Giovanelli, R. : 1997, *Galaxy scalling relations, ESO astrophysics symposia*, Proc. of the ESO workshop, eds. L. N. da Costa and A. Renzini, Sprnger, p. 146.

Karachentsev, I. D., Georgiev, Ts. B., Kajsin, S. S., Kopylov, A. I., Ryadchenko, V. P., and Shergin, V. S. : 1992, *Astron. Astrophys. Transactions*, **2**, 256.

Karachentsev, I. D., Karachentseva, V. E., Kudrya, Yu. N., Sharina, M. E., Parnovsky, S. L. : 1999, *Bull. Spec. Astrophys. Obs.*, **47**, 5.

Karachentsev, I. D, Makarov, D. A. : 1996, *Astron. J.*, **111**, 794.

Larson, R. B., 1976, *Mon. Not. Royal Astron. Soc.*, **176**, 31.

Pohlen, M., Dettmar, R. J., Luetticke, R., Schwarzkopf, U. : 2000, *Astron. Astrophys.*, **144**, 405.

van der Kruit, P. C., Searle, L. : 1981, *Astron. Astrophys.*, **95**, 105.